Investigation of Sm3+ -doped PBNaG glasses for orange LED applications

by Abd Hakim S

Investigation of Sm^{3+}-doped PBNaG glasses for orange LED applications

Juniastel Rajagukguk, Nursaida Harahap, Rappel Situmorang & S. Abd Hakim

ONLINE FIRST

Journal of the Korean Physical Society

ISSN 0374-4884

J. Korean Phys. Soc.
DOI 10.1007/s40042-020-00034-6

Springer

Journal of the Korean Physical Society
https://doi.org/10.1007/s40042-020-00034-6

Online ISSN 1976-8524
Print ISSN 0374-4884

ORIGINAL PAPER

Investigation of Sm^{3+}-doped PBNaG glasses for orange LED applications

Juniastel Rajagukguk[1] · Nursaida Harahap[1] · Rappel Situmorang[1] · S. Abd Hakim[1]

Received: 9 September 2020 / Revised: 20 October 2020 / Accepted: 9 November 2020

Abstract

The doping of a host glass with rare-earth ions is quite interesting when investigating their wide applications in several fields, such as laser and optical fibers. In this study, the glass medium had a composition of $(70-x)$ P_2O_5–$10Bi_2O_3$–$10Na_2O$–$10Gd_2O_3$–xSm_2O_3 with $x=0$, 0.05, 0.1, 0.5, 1.0, 3.0 mol% and were fabricated using melt-quenching method. The optical properties of Sm^{3+}-doped samples with different Sm^{3+} concentrations were determined by measuring the absorption and luminescence spectra in the visible light region. Both the direct and the indirect bandgap energies were slightly decreased after doping with Sm^{3+} ions. The maximum experimental oscillator strength was 3.65×10^{-6} for the band transition $^6H_{5/2}\rightarrow{}^6F_{7/2}$ over glass PBNaGSm5. The Judd–Ofelt parameters were applied to evaluate the properties of glass samples. The highest emission intensity was located in the orange range with a wavelength of 597 nm under an excitation wavelength of 401 nm. An obvious decrease in the lifetime was observed at higher Sm^{3+} ion concentrations.

Keywords Optic glass · Phosphate · Samarium · Orange emission · Lifetime

1 Introduction

Glasses doped with rare earth elements have greatly attracted the attention of researchers due to their wide applications as optical fibers, laser materials, fluorescence screens, optical detectors, and waveguides [1–5]. Some previous works have investigated the effect of the samarium ion doped into different host glasses [6–11]. Phosphate glass is one of the most suitable hosts because it has high mechanical properties and high thermal stability [12]. In general, the thermal expansions of phosphate glasses are higher while the transition temperatures are lower than those of silicate or borate glasses [13]. Furthermore, rare earth ions are more soluble in phosphate glass than they are in telluride glass, leading to a higher luminescence quantum yield [14]. The rare-earth of trivalent samarium ion (Sm^{3+}) is one of the most interesting RE ions to investigate because its $^4G_{5/2}$ emission level has a high quantum efficiency and different emission channels [15, 16]. Sm^{3+}shows strong luminescence in the orange–red spectra region, which is useful for high-density optical data storage, color display and underwater communication applications.

The addition of sodium oxide (Na_2O) to a host glass can increase the glass transition temperature (Tg), eventually leading to higher thermal stability [17]. Moreover, Na_2O is added to increase homogenization, to reduce the melting point of the glass host, and to reduce the glass damage and bubbles [18, 19]. This present work investigates the effect of the Sm^{3+} active ion concentration on the optical properties of glass phosphate and obtain the values of the Judd–Ofelt parameters.

2 Experimental

Sm^{3+}-doped phosphate bismuth sodium gadolinium was prepared using the melt-quenching technique as in our previous work [20]. The chemical composition of the glass was $(70-x)P_2O_5$-$10Bi_2O_3$–$10Na_2$–$10Gd_2O_3$–xSm_2O_3, where $x=0.05$, 0.1, 0.5, 1.0 and 3.0 mol%, where denoted as PBNaGS1, PBNaGS2, PBNaGS3, PBNaGS4 and PBNaGS5. The chemical compounds P_2O_5, Bi_2O_3, Na_2O, Gd_2O_3, and Sm_2O_3 were directly used as raw materials without a purification step. Those chemicals were then mixed homogeneously in alumina crucibles, after that, the alumina crucibles

✉ Juniastel Rajagukguk
juniastel@unimed.ac.id

1 Department of Physics, Faculty of Mathematics and Natural Sciences, Universitas Negeri Medan, Medan, Indonesia

Published online: 15 December 2020

containing the materials were inserted into an electric furnace and heated from room temperature to 1200 °C with a holding time of 2 h. After the raw materials had melted, the alumina crucible was lifted and immediately poured into a stainless-steel mold that had been pre-heated to 500 °C and held at that temperature for another 2 h. Finally, the samples were allowed to slowly cool to room temperature. Before the measurements of the optical and radiative properties, the glass samples were cut and polished ($2 \times 1.5 \times 1$ cm^3). The optical absorption spectra were recorded using a UV–Vis-NIR spectrophotometer (UV-3600 Shimadzu). The fluorescence spectra were analyzed using a PTI Quanta Master series (QM-300) spectrofluorometer.

3 Results and discussion

3.1 Absorption spectra

The absorption spectra of the Sm^{3+}-doped phosphate glasses were recorded using an UV–VIS spectrophotometer in the range from 400 to 1800 nm, and the results are presented in Fig. 1. Clearly, the absorbance bands are gradually enhanced with increasing Sm^{3+} concentration. Those bands are located at 436, 471, 946, 1080, 1233, 1379, 1486, 1535, 1592 nm and are related to transitions of the ground energy level: ${}^6H_{5/2}$ to ${}^4G_{9/2}$, ${}^4I_{11/2}$, ${}^6F_{11/2}$, ${}^6F_{9/2}$, ${}^6F_{7/2}$, ${}^6F_{5/2}$, ${}^6F_{3/2}$, ${}^6H_{15/2}$, and ${}^6F_{1/2}$, respectively.

The optical properties of the Sm^{3+}-doped phosphate glasses were investigated using Tauc's Plot to calculate the bandgap energies. Figures 2 and 3 exhibit its indirect and direct bandgap energies, respectively. The indirect band energy is found to be lower by 0.4 eV after doping with 1% mol Sm^{3+}. The indirect bandgap energies of PBNaGS1, PBNaGS2, PBNaGS3, PBNaGS4 and PBNaGS5 are 3.20, 3.00, 2.90, 2.80 and 3.10 eV, respectively. Similarly, the direct bandgap energy values of Sm^{3+}-doped phosphate glasses were also decreased after doping. Their values were 3.42, 3.35, 3.29, 3.24 and 3.37 eV for PBNaGS1, PBNaGS2, PBNaGS3, PBNaGS4 and PBNaGS5, respectively. The indirect and the direct bandgap energies exhibited similar trends, where their values decreased with increasing concentration to an optimum of 1 mol % (PBNaGS4). With further increasing the concentration to 3 mol % (PBNaGS5), the bandgap values slightly increased. The variations of bandgap energies due to the creation of defects and changes in the composition of the glass after doping which were similar to those in our previous reports [20, 21].

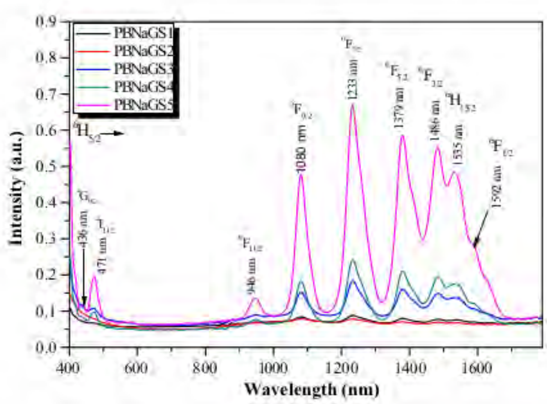

Fig. 1 Absorption spectra for glasses Sm: phosphate with different Sm^{3+} ion concentrations

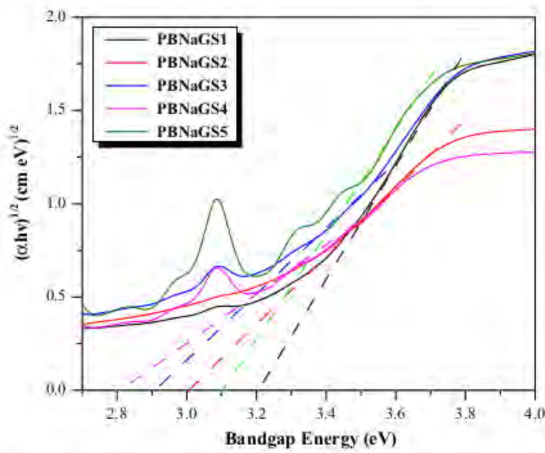

Fig. 2 Indirect bandgap energy for glasses Sm: phosphate with different Sm^{3+} ion concentrations

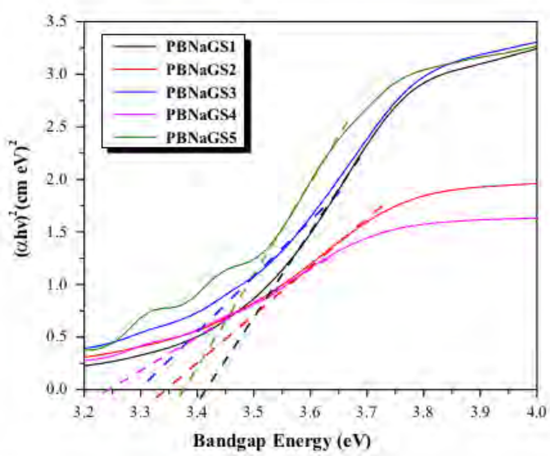

Fig. 3 Direct bandgap energy for glasses Sm: phosphate with different Sm^{3+} ion concentrations

Table 1 Experimental (f_{exp}) and calculated (f_{cal}) oscillator strength ($\times 10^{-6}$) of Sm: phosphate with different Sm^{3+} ion concentrations

Transition	PBNaGSm1		PBNaGSm2		PBNaGSm3		PBNaGSm4		PBNaGSm5	
$^6H_{5/2} \rightarrow$	f_{exp}	f_{cal}	f_{exp}	f_{cal}	f_{exp}	f_{cal}	f_{exp}	f_{cal}	f_{exp}	f_{cal}
$^4G_{9/2}$	–	0.05	–	0.05	–	0.05	–	0.05	0.45	0.05
$^4I_{11/2}$	–	0.11	–	0.11	0.86	0.11	0.87	0.11	5.62	0.12
$^6F_{11/2}$	–	0.28	–	0.27	0.13	0.28	0.11	0.28	0.97	0.28
$^6F_{9/2}$	0.15	1.72	0.003	1.71	0.55	1.71	0.64	1.71	3.60	1.72
$^6F_{7/2}$	0.14	2.61	0.0006	2.61	0.63	2.61	0.70	2.61	3.95	2.60
$^6F_{5/2}$	0.09	1.89	0.0001	1.89	0.33	1.89	0.38	1.89	2.12	1.89
$^6F_{3/2}$	0.04	2.28	–	2.29	0.13	2.28	0.15	2.29	0.85	2.31
$^6H_{15/2}$	–	0.01	–	0.01	0.08	0.01	0.08	0.01	0.46	0.01
$^6F_{1/2}$	–	2.09	–	2.09	–	2.09	–	2.09	0.03	2.10
Δf_{rms}	±2.0		±1.2		±1.6		±1.8		±1.0	

Table 2 Judd–Ofelt parameter values ($\times 10^{-20}$ cm^2) and spectroscopy quality factors (χ) for glass Sm: phosphate with different Sm^{3+} ion concentrations

Glass	Ω_2	Ω_4	Ω_6	$\chi(\Omega_4/\Omega_6)$
PBNaGSm1	6.1322	2.6495	0.1832	14.462
PBNaGSm2	6.1263	2.6601	0.18311	14.527
PBNaGSm3	6.1010	0.26665	0.18296	1.4574
PBNaGSm4	6.1263	0.26601	0.18311	1.4527
PBNaGSm5	6.2641	0.26208	0.18387	1.4253

3.2 Field strength and Judd–Ofelt analysis

The experimental and the calculated oscillator strengths were determined according to equations in the Ref. [22], and the results are listed in Table 1. Clearly both the calculated and the experimental oscillator strengths decrease significantly with increasing Sm^{3+} concentrations. The maximum experimental oscillator strength was achieved for the PBNaGSm5 glass with a value of 3.65×10^{-6} for the band transition $^6H_{5/2} \rightarrow {}^6F_{7/2}$. For a validation of the quality of the spectra intensity, the root-mean-square deviation (δ_{rms}) was calculated for fittings of the experimental and the calculated oscillator strengths. In this case, the small rms deviations value corresponds to the reliable calculation. The rms deviations for PBNaGS1, PBNaGS2, PBNaGS3, PBNaGS4 and PBNaGS5 were 2.0, 1.2, 1.6, 1.8, and 1.0×10^{-6}, respectively. Those values are in good agreement with the data limit.

Table 2 lists the Judd–Ofelt parameters and spectroscopy quality factors for Sm^{3+}-doped phosphate glass with different Sm^{3+} contents. Clearly, all glass samples followed the order $\Omega_2 > \Omega_4 > \Omega_6$. According to the literature [23], glass samples with higher values of Ω_2 and Ω_4 but lower Ω_6 are considered to be good hosts because they can produce a high luminescence intensity ratio. In general, the Ω_6 parameter corresponds to the rigidity of the host glass. The Ω_6 values did not change with increasing Sm^{3+} content even up to 3 mol%. This indicates that that the rigidity does not change. The highest spectroscopy quality factor was 14.527 for the PBNaGSm2 sample. However, with further addition of Sm^{3+}, not only did the JO parameters decrease but also the spectroscopy quality factor significantly decreased.

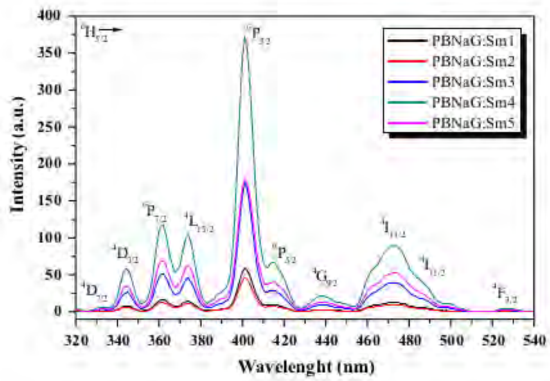

Fig. 4 Excitation spectra of Sm: phosphate with different Sm^{3+} ion concentrations

3.3 Excitation spectra

The excitation wavelength is well known to be crucial to obtain efficient luminescence properties and to record the energy level transitions. Thus, the excitation spectra of Sm: phosphate were recorded in the wavelength range from 320 to 540 nm under an emission wavelength of 600 nm. As shown in Fig. 4, ten excitations bands located at 332, 344, 361,374, 401, 416, 440, 472, 490 and 527 nm which are related to $^6H_{5/2} \rightarrow {}^4D_{7/2}$, $^6H_{5/2} \rightarrow {}^4D_{3/2}$, $^6H_{5/2} \rightarrow {}^6P_{7/2}$, $^6H_{5/2} \rightarrow {}^4L_{15/2}$, $^6H_{5/2} \rightarrow {}^6P_{3/2}$, $^6H_{5/2} \rightarrow {}^6P5_{/2}$, $^6H_{5/2} \rightarrow {}^4G_{9/2}$, $^6H_{5/2} \rightarrow {}^4I_{13/2}$, $^6H_{5/2} \rightarrow {}^4I_{11/2}$ and $^6H_{5/2} \rightarrow {}^4F_{3/2}$ transition, respectively, where recorded clearly from Fig. 4, the intensity of excitation gradually increases with increasing concentration of Sm^{3+} up to 1 mol % (PBNaGSm4), after further increases the amount of Sm^3 to 3 mol% (PBNaGSm5) lead to a sharp decrease in the excitation intensity 50% as compared to the highest one (PBNaGSm4). In addition, the excitation located at a wavelength of 402 nm had the highest intensity among those ten bands.

3.4 Luminescence properties

Figure 5 shows the luminescence properties of Sm: phosphate medium glass in the spectral range from 550 to 720 nm with an excitation wavelength (λ_{ex}) of 401 nm. Four emission band transitions are observable for all the glass samples, as clearly shown in Fig. 5. Those bands are located at 562, 597, 644, and 703 nm and corresponds to the transitions of $^4G_{5/2} \rightarrow {}^6H_{5/2}$, $^4G_{5/2} \rightarrow {}^6H_{7/2}$, $^4G_{5/2} \rightarrow {}^6H_{9/2}$, and $^4G_{5/2} \rightarrow {}^6H_{11/2}$, respectively. No significant difference in the emission intensity was observed for low concentrations 0.05 and 0.1 mol%, of Sm^{3+}. However, when the concentration was increased to 0.5 mol% (PBNaGSm3), the emission intensity significantly increased. The highest emission intensity was reached for 1 mol% Sm^{3+} doping (PBNaGSm4). Similar to the excitation result in the previous section, the emission intensity also started to decrease when the concentration of Sm^{3+} ion was increased to 3 mol % (PBNaGSm5). The decrease in the intensity after doping at a certain level is well known in the field due to more interactions RE to RE ions and RE ions to the host glass, which causes cross-relaxation in the active ion centers via concentration quenching [24]. Among these four emission bands, the transition of $^4G_{5/2} \rightarrow {}^6H_{7/2}$ at a wavelength of 597 nm obviously is the most intense. This wavelength is in the range of orange (590—625 nm). Therefore, this present glass sample has a potential application for an orange LED.

3.5 Decay curve analysis

Figure 6 shows the emission decay process for transitions with an excitation wavelength of 400 nm. The decay process has a non-exponential nature due to cross-relaxation through multi-polar interactions between Sm^{3+} ions. The lifetimes of the energy levels can be determined experimentally by measuring the emission decay from each of the $^4G_{5/2} \rightarrow {}^6H_{7/2}$ transitions [25, 26]. When Sm^{3+} is excited by an excitation wavelength, a relaxation non-radiation rapidly extends to fluorescent energy levels because of the gap energy [27]. Orange luminescence was produced from a strong band located at a wavelength of about 600 nm. The decay curves of the $^4G_{5/2} \rightarrow {}^6H_{7/2}$ (600 nm) transition for different concentrations of Sm^{3+} were seem to have a single exponential character for PBNaG:Sm1 to PBNaGS4 and a double exponential for Sm^{3+} higher concentration (PBNaGS5). The lifetime reduction phenomenon from single exponential to double exponential leads to a concentration quenching effect in the energy state of the $^4G_{5/2}$ level in PBNaGS5 glass (3.0 mol% concentration). The single exponential form appears to be the energy transfer from cross-relaxation processes among Sm^{3+} ions. The lifetimes for PBNaGS1, PBNaGS2, PBNaGS3, PBNaGS4 and PBNaGS5 were 2.67, 2.66, 2.06, 1.61, and 0.68 ms, respectively. Obviously, the lifetime significantly decreased by adding high concentrations of Sm^{3+} due to the low probability of non-radiative relaxations.

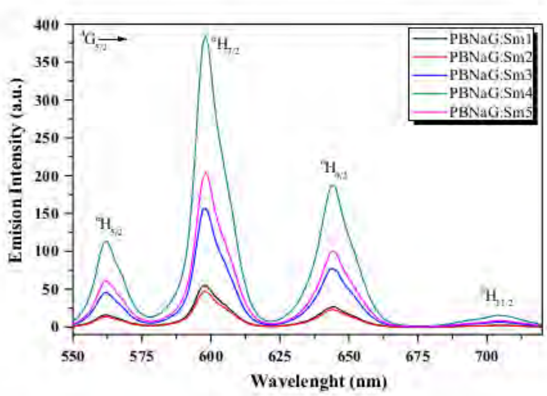

Fig. 5 Emission spectra of Sm: phosphate with different Sm^{3+} ion concentrations

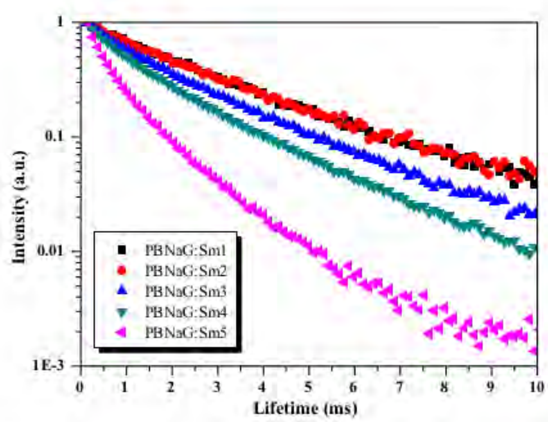

Fig. 6 Decay profiles of the $^4G_{5/2} \rightarrow {}^6H_{7/2}$ for different Sm^{3+} ion concentrations doped phosphate glass

4 Conclusion

Sm^{3+}-doped glass medium has been successfully designed and characterized using optical and radiative analyses. We found that the absorbance band was significantly enhanced and that bandgap energies slightly decreased with increasing Sm^{3+} concentrations. The Judd–Ofelt parameters of the glass samples followed the order $\Omega_2 > \Omega_4 > \Omega_6$. The maximum experimental oscillator strength was 3.65×10^{-6} for the band transition $^6H_{5/2} \rightarrow {}^6F_{7/2}$ in the PBNaGSm5 glass. Under an excitation wavelength of 401 nm, four emission bands were observed in the visible-light region. Among them, the transition of $^4G_{5/2} \rightarrow {}^6H_{7/2}$ with a peak wavelength of 597 nm showed the highest intensity. The lifetime was obviously lower at higher concentrations of Sm^{3+} due to the low probability of non-radiative relaxations. This glass sample has potential applications for an orange LED.

Acknowledgements This work was supported by Directorate General of Research Enhancement and Development of the Republic of Indonesia under contract number 0445/UN33/KEP/PPL/2020.

References

1. H. Lin, W. Qin, J. Zhang, C. Wu, Solid State Commun. **141**, 436 (2007)
2. Y.L.P. Reddy, M. Waaiz, C.K. Reddy, Int. J Pure Appl. Phys. **13**(2), 249 (2017)
3. S.Q. Mawlud, Spectrochim. Acta A Mol. Biomol. Spectrosc. **209**, 78 (2019)
4. S. Thomas, M.L. Chithambo, Radiat. Measure **120**, 83 (2018)
5. I.I. Kindrat, B.V. Padlyak, B. Kukliński, A. Drzewiecki, V.T. Adamiv, J. Lumin. **213**, 290 (2019)
6. M.E. Alvarez-Ramos, R.C. Carrillo-Torres, R. Sánchez-Zeferino, U. Caldiño, J. Alvarado-Rivera, J. Non-Cryst. Solids **521**, 119462 (2019)
7. F. Steudel, S. Loos, B. Ahrens, S. Schweizer, J Lumin. **170**, 770 (2016)
8. S. Thomas, M.L. Chithambo, Rad. Measure **120**, 83 (2018)
9. Z. Mazurak, S. Bodył, R. Lisiecki, J. Gabryś-Pisarska, M. Czaja, Opt. Mater. **32**(4), 547 (2010)
10. N. Wantana, S. Kaewjaeng, S. Kothan, H.J. Kim, J. Kaewkhao, J. Lumin. **181**, 382 (2017)
11. X.Y. Sun, D.G. Jiang, Y.Z. Sun, X. Zhang, Q.L. Hu, Y. Huang, Y. Tao, J. Non-Cryst. Solids **389**, 72 (2014)
12. W. Jia, C. Su, Y. Wei, H. Zhang, X. Zou, J. Lumin. **215**, 116576 (2019)
13. K. J. D. MacKenzie, M. E. Smith, Chapter 7—NMR of Other Commonly Studied Nuclei. In: *Pergamon Materials Series*, Pergamon 6:399 (2002)
14. M.M. Ismail, I.K. Batisha, L. Zur, A. Chiasera, M. Ferrari, A. Lukowiak, Opt. Mater. **99**, 109591 (2020)
15. T. Srihari, C.K. Jayasankar, Optic. Mater. **66**, 35 (2017)
16. N. Chanthima, Y. Tariwong, M. Djamal, J. Kaewkhao, N. Sangwaranatee, Mater. Today Proc. **5**(7), 15066 (2018)
17. R. Pavai, P. Dharsini, IOSR, J. Appl. Phys. **09**, 67 (2017)
18. P. Chimalawong, J. Kaewkhao, T. Kittiauchawal, C. Kedkaew, P. Limsuwan, J. Appl. Sci. **7**(4), 584 (2010)
19. W.Z. Tawfik, M.M. Mahdy, M.A.K. Elfayoumi, M.M. Elokr, J. Alloys Compd. **509**(41), 10070 (2011)
20. J. Rajagukguk, R. Situmorang, M. Djamal, R. Rajaramakrishna, J. Kaewkhao, P.H. Minh, J. Lumin. **216**, 116738 (2019)
21. J. Rajagukguk, B. Sinaga, J. Kaewkhao, Spectrochim. Acta A Mol. Biomol. Spectrosc. **223**, 117342 (2019)
22. G. Neelima, V.K. Kummara, N. Ravi, K. Suresh, S.N. Rasool, K. Tyagarajan, T.J. Prasad, Mater. Res. Bull **110**, 223 (2019)
23. N. Vijaya, P. Babu, V. Venkatramu, C. Jayasankar, S. León-Luis, U. Rodríguez-Mendoza, I. Martín, V. Lavín, Sens. Actuators B Chem. **186**, 156 (2013)
24. N. Deopa, A.S. Rao, M. Gupta, G. Vijaya Prakash, Optic Mater. **75**, 127 (2018)
25. L. Yuliantini, M. Djamal, R. Hidayat, K. Boonin, P. Yasaka, E. Kaewnuam, J. Kaewkhao, J. Lumin. **213**, 19 (2019)
26. A. Herrera, A. Becerra, N.M. Balzaretti, J. Lumin. **188**, 193 (2017)
27. G. Neelima, V.K. Kummara, N. Ravi, K. Suresh, S.N. Rasool, K. Tyagarajan, T.J. Prasad, Mater. Res. Bull. **110**, 223 (2019)

Publisher's Note Springer Nature remains neutral with regard to jurisdictional claims in published maps and institutional affiliations.

Investigation of Sm3+ -doped PBNaG glasses for orange LED applications

ORIGINALITY REPORT

16%	4%	15%	3%
SIMILARITY INDEX	INTERNET SOURCES	PUBLICATIONS	STUDENT PAPERS

PRIMARY SOURCES

1	Submitted to BENEMERITA UNIVERSIDAD AUTONOMA DE PUEBLA BIBLIOTECA Student Paper	1%
2	A. Herrera, A. Becerra, N.M. Balzaretti. "Novel NIR emission 4 G 5/2 to 6 F 11/2 and efficient multichannel emissions of Sm 3+ doped GeO 2 -PbO glass", Journal of Luminescence, 2017 Publication	1%
3	J. Rajagukguk, C.S. Sarumaha, N. Chanthima, N. Wantana, S. Kothan, N. Wongdamnern, J. Kaewkhao. "Radio and Photo Luminescence of Dy3+ Doped Lithium Fluorophosphate Scintillating Glass", Radiation Physics and Chemistry, 2021 Publication	1%
4	Bilir, G.. "Judd-Ofelt analysis and near infrared emission properties of the Er^3^+ ions in tellurite glasses containing WO"3 and CdO", Optics Communications, 20110201 Publication	1%

5	Submitted to Institute of International Studies Student Paper	1 %
6	zh.scientific.net Internet Source	1 %
7	P. Chimalawong, K. Kirdsiri, J. Kaewkhao, P. Limsuwan. "Investigation on the Physical and Optical Properties of Dy3+ Doped Soda-Lime-Silicate Glasses", Procedia Engineering, 2012 Publication	1 %
8	Selvaraju, K., N. Vijaya, K. Marimuthu, and V. Lavin. "Composition dependent spectroscopic properties of Er^{3+} -doped boro-tellurite glasses", physica status solidi (a), 2013. Publication	1 %
9	A. A. El-Maaref, R. M. El-Agmy, Kh. S. Shaaban, E. A. Abdel Wahab. "Optical and spectroscopic study of Nd2O3-doped SBN glass in the near-infrared, visible and UV regions under pumping up-conversion emissions", The European Physical Journal Plus, 2021 Publication	1 %
10	I. Jlassi, S. Mnasri, H. Elhouichet. "Concentration dependent spectroscopic behavior of Sm 3+ -doped sodium fluoro-phosphates glasses for orange and reddish-orange light emitting applications", Journal of Luminescence, 2018	1 %

Publication

11	M.S.A. Mohd Saidi, S.K. Ghoshal, R. Arifin, M.K. Roslan, R. Muhammad, W.N.W. Shamsuri, M. Abdullah, M.S. Shaharin. "Spectroscopic properties of Dy 3+ doped tellurite glass with Ag/TiO 2 nanoparticles inclusion: Judd−Ofelt analysis", Journal of Alloys and Compounds, 2018 Publication	1 %
12	jurnal.ar-raniry.ac.id Internet Source	1 %
13	wiki.uef.fi Internet Source	1 %
14	Kindrat, I.I., B.V. Padlyak, and A. Drzewiecki. "Luminescence properties of the Sm-doped borate glasses", Journal of Luminescence, 2015. Publication	<1 %
15	iopscience.iop.org Internet Source	<1 %
16	R Situmorang, Rahmaniar, D D. Panggabean, C. Sarumaha, J Kaewkhao, Sunaryono, J Rajagukguk. " The Dy O Effect Study on Spectroscopy and Optical Properties of PbiNaGd Glass for Optical Amplification ", Journal of Physics: Conference Series, 2020 Publication	<1 %

17	Dongdong Qin, Xiaozhen Ma, Bao Zhang, Qing Luo, Haining Na, Jing Chen, Jin Zhu. "Ultra-high gas barrier and enhanced mechanical properties of corn cellulose nanocomposite films filled with graphene oxide nanosheets", Carbohydrate Polymer Technologies and Applications, 2021 Publication	<1 %
18	Farouk, M.. "Effect of TiO2 on the structural, thermal and optical properties of BaO–Li2O–diborate glasses", Journal of Non-Crystalline Solids, 2014. Publication	<1 %
19	G. Lakshminarayana, Kawa M. Kaky, S.O. Baki, Song Ye, A. Lira, I.V. Kityk, M.A. Mahdi. "Concentration dependent structural, thermal, and optical features of Pr 3+ -doped multicomponent tellurite glasses", Journal of Alloys and Compounds, 2016 Publication	<1 %
20	Youjie Hua, Jun Sun, Hongping Ma, Renguang Ye, Feifei Huang, Shiqing Xu. "Optimization of tellurite glass system toward enhanced luminescence of phosphor solids for white LEDs", Optical Materials, 2021 Publication	<1 %
21	www.sciencegate.app Internet Source	<1 %

22	Ataullah, I. Khan, S. Khattak, M. Shoaib, J. Kaewkhao, I. Ullah, G. Rooh. "Spectral investigation of lithium-telluride based glasses doped with Sm3+-ions for lighting application", Journal of Alloys and Compounds, 2021 Publication	<1 %
23	Karthikeyan, B.. "Novel synthesis and optical properties of Sm^3^+ doped Au- polyvinyl alcohol nanocomposite films", Chemical Physics Letters, 20061211 Publication	<1 %
24	Karunakaran, R.T.. "Structural, optical and thermal investigations on Dy^3^+ doped NaF-Li"2O-B"2O"3 glasses", Physica B: Physics of Condensed Matter, 20091115 Publication	<1 %
25	M.N. Ami Hazlin, M.K. Halimah, F.D. Muhammad. "Absorption and emission analysis of zinc borotellurite glass doped with dysprosium oxide nanoparticles for generation of white light", Journal of Luminescence, 2018 Publication	<1 %
26	Seungwan Lee. "Respiratory-correlated 4D digital tomosynthesis with deep convolutional neural networks for image-guided radiation	<1 %

therapy", Journal of the Korean Physical Society, 2021
Publication

27	Suresh Kumar, J.. "Photoluminescence and energy transfer properties of Sm^3^+ doped CFB glasses", Solid State Sciences, 201108 Publication	<1 %
28	Wafa Hami, Mohamed Daoud, Daniel Zambon, Mohamed Elaatmani, Abdelouahad Zegzouti. "Synthesis and characterization of AgYP2O7 pyrophosphate activated with Tb3+, Sm3+ and Dy3+ ions", Inorganic Chemistry Communications, 2019 Publication	<1 %
29	dyuthi.cusat.ac.in Internet Source	<1 %
30	"NMR of Other Commonly Studied Nuclei", Elsevier BV, 2002 Publication	<1 %
31	Agarwal, A.. "Judd-Ofelt parameters and radiative properties of Sm^3^+ ions doped zinc bismuth borate glasses", Optical Materials, 200912 Publication	<1 %
32	Chun-Xiao Liu, He Pan, Jing-Yan Lv, Jing-Yi Chen, She-Bao Lin, Rui-Lin Zheng, Li-Li Fu, Liao-Lin Zhang. "An infrared 2D Nd3+-doped	<1 %

phosphate glass waveguide formed by proton implantation and femtosecond laser ablation", Infrared Physics & Technology, 2021
Publication

33	Culea, E.. "Structural and physical characteristics of CeO"2-GeO"2-PbO glasses and glass ceramics", Journal of Alloys and Compounds, 20100903 Publication	<1 %
34	Hui-Wen Lee, Katharine T. Briggs, John P. Marino. "Dissecting structural transitions in the HIV-1 dimerization initiation site RNA using 2-aminopurine fluorescence", Methods, 2009 Publication	<1 %
35	Saif, M.. "Titanium dioxide nanomaterial doped with trivalent lanthanide ions of Tb, Eu and Sm: Preparation, characterization and potential applications", Inorganica Chimica Acta, 20070610 Publication	<1 %
36	uwe-repository.worktribe.com Internet Source	<1 %
37	Jayasimhadri, M.. "Spectroscopic characteristics of Sm^3^+-doped alkali fluorophosphate glasses", Spectrochimica Acta Part A: Molecular and Biomolecular Spectroscopy, 200607	<1 %

Publication

38	A.U. Ahmad, S. Hashim, S.K. Goshal. "Optical traits of neodymium-doped new types of borate glasses: Judd-Ofelt analysis", Optik, 2019 Publication	<1 %
39	B.C. Jamalaiah, J. Suresh Kumar, A. Mohan Babu, T. Suhasini, L. Rama Moorthy. "Photoluminescence properties of Sm3+ in LBTAF glasses", Journal of Luminescence, 2009 Publication	<1 %
40	Jinjoo Park. "Fabrication of wide-gap p-type microcrystalline silicon-oxide emitter induced high built-in potential in heterojunction solar cells", Journal of the Korean Physical Society, 2020 Publication	<1 %
41	N. Wantana, Y. Ruangtaweep, E. Kaewnuam, S.C. Kang, H.J. Kim, S. Kothan, J. Kaewkhao. "Development of WO3-Gd2O3 B2O3 high density glasses doped with Dy3+ for photonics and scintillation materials application", Solid State Sciences, 2020 Publication	<1 %

Exclude quotes	Off	Exclude matches	Off
Exclude bibliography	On		

Investigation of Sm3+ -doped PBNaG glasses for orange LED applications

GRADEMARK REPORT

FINAL GRADE

/0

GENERAL COMMENTS

Instructor

PAGE 1

PAGE 2

PAGE 3

PAGE 4

PAGE 5

PAGE 6

PAGE 7